JVI Journals.ASM.org

Two Novel Proteins of Cyanophage Syn5 Compose Its Unusual Horn Structure

Desislava A. Raytcheva,[a] Cameron Haase-Pettingell,[b] Jacqueline Piret,[a] Jonathan A. King[b]

Department of Biology, Northeastern University, Boston, Massachusetts, USA[a]; Department of Biology, Massachusetts Institute of Technology, Cambridge, Massachusetts, USA[b]

The marine cyanophage Syn5 can be propagated to a high titer in the laboratory on marine photosynthetic *Synechococcus* sp. strain WH8109. The purified particles carry a novel slender horn structure projecting from the vertex opposite the tail vertex. The genome of Syn5 includes a number of genes coding for novel proteins. Using immune-electron microscopy with gold-labeled antibodies, we show that two of these novel proteins, products of genes 53 and 54, are part of the horn structure. A third novel protein, the product of gene 58, is assembled onto the icosahedral capsid lattice. Characterization of radioactively labeled precursor procapsids by sucrose gradient centrifugation shows that there appear to be three classes of particles—procapsids, scaffold-deficient procapsids, and expanded capsids. These lack fully assembled horn appendages. The horn presumably assembles onto the virion just before or after DNA packaging. Antibodies raised to the recombinant novel Syn5 proteins did not interfere with phage infectivity, suggesting that the functions of these proteins are not directly involved in phage attachment or infection of the host WH8109. The horn structure may represent some adaption to the marine environment, whose function will require additional investigation.

Marine photosynthetic cyanobacteria are at the base of the food chain in the world's oceans and contribute to the global carbon cycle. Bacteriophages infecting these cells are ubiquitous in the marine environment, playing a role in nutrient recycling, host population dynamics and diversity, and probably gene transfer. Some cyanophages carry host photosynthetic genes that are expressed during phage infection (1, 2). Many marine bacteriophages exhibit capsid appendages not seen in enteric phages, such as the horn of Syn5 (3, 4).

Syn5 is a double-stranded DNA (dsDNA), short-tailed marine bacteriophage isolated from the Sargasso Sea (5). Its laboratory host is the cyanobacterial *Synechococcus* sp. strain WH8109 (5, 6). Syn5 has a 46,214-bp genome, including an RNA polymerase gene (7). The genome shares high synteny with T7 and with several cyanophages, especially *Synechococcus* bacteriophage P60 and *Prochlorococcus* phage P-SSP7. Mass spectrometry (MS) of the gel-excised structural protein bands of Syn5 initially identified 13 proteins closely resembling proteins found in other dsDNA phages, including the coat and portal proteins, three internal core proteins, and the tail apparatus components (7). However, at least four Syn5 proteins—gp53, gp54, gp55, and gp57—were novel in that their sequences did not match other sequences in the NCBI database at the time of sequencing (BLASTp; E value of <0.001). The C-terminal domain of a fifth novel protein, gp58, is a good match to the C-terminal domain of a structural protein in the newly sequenced genome of the *Synechococcus* siphovirus S-CBS2.

Electron microscopy (EM) of Syn5 shows an icosahedral virion, with a head diameter of 60 nm and a short tail (7), which assembles through a procapsid intermediate lacking condensed DNA (8). The procapsid and a class of expanded capsids have been recently directly visualized within infected cells by cryo-electron tomography (cryo-ET) (9).

Cyanobacteria and cyanophage are presumed to have evolved prior to the emergence of terrestrial organisms (10). The Syn5 feature of assembling the capsid by first forming a procapsid empty of DNA and subsequently filling it with genomic DNA suggests that this assembly pathway evolved in the marine environment, perhaps in cyanophage, and gave rise to the assembly pathway for enteric dsDNA phages and viruses.

The isolated mature Syn5 capsid exhibits knob-like outer capsid structures, which lie across each hexamer. Cryo-electron microscopy (cryo-EM) reveals a novel long, slender horn-like structure positioned on the vertex opposite the tail (Fig. 1A). The horn is 30 to 35 nm in length, 10 nm wide at its base, and 2 to 3 nm wide at its tip, and only one is observed per particle. It is flexible and is often observed to be bent at the base (Fig. 1A). Prior to the cryo-EM of Syn5, only two other bacteriophages were reported with appendages attached opposite the tail (11). Recently, a fourth example, the *Myoviridae* cyanophage Bellamy, was also found to have a tail-like appendage opposite the tail (Welkin Pope and Roger Hendrix, personal communication).

The purpose of the experiments described here was to address the roles of the novel Syn5 proteins. Two of these, gp53 (48 kDa) and gp54 (65 kDa), are larger than the other three and are the primary candidates for the horn structure. The smaller proteins (gp55, gp57, and gp58) are good candidates for the outer capsid knob proteins. The genes for three of these, gp53, gp54, and gp58, were cloned, the proteins were overexpressed and purified, and polyclonal antibodies were raised against them (8, 12). These antibodies were used in immunogold labeling to analyze which virion structural components are composed of the novel proteins. The antibodies were also used in neutralization assays to test their effects, if any, on phage infectivity. Radiolabeled amino acids were used to follow *de novo* synthesis of Syn5 proteins during infection

Received 29 August 2013 **Accepted** 26 November 2013
Published ahead of print 4 December 2013
Address correspondence to Jonathan A. King, jaking@mit.edu.

doi:10.1128/JVI.02479-13

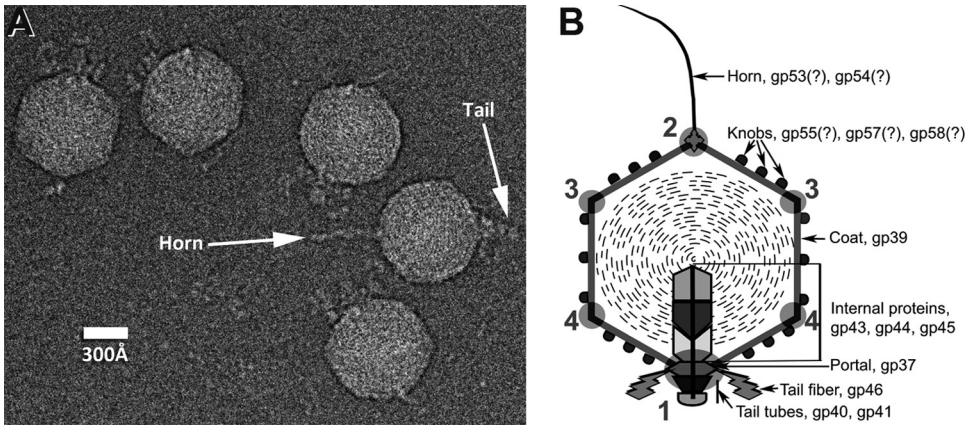

FIG 1 Images of phage Syn5. (A) Cryo-EM image of Syn5. The horn and tail are labeled on one phage (Preeti Gipson, Baylor School of Medicine). (B) Schematic drawing of Syn5 with major structures labeled and each vertex assigned a number to facilitate the discussion of the gold bead labeling data. (Reprinted from reference 8.)

to determine the assembly stages at which the novel proteins are added.

MATERIALS AND METHODS

Immunogold labeling of Syn5 with anti-Syn5, anti-gp53, anti-gp54, and anti-gp58 antibodies. The genes of three of the Syn5 novel proteins—gp53, gp54, and gp58—were cloned, and the proteins were overexpressed and purified. These proteins were injected in rabbits (12), and the resulting antibodies were used as primary antibodies. The anti-Syn5 antibodies were prepared earlier (7). The secondary antibodies were gold-labeled goat anti-rabbit IgG(H+L) F(ab′)2 (AH, conjugate absorbed against human serum proteins) (10-nm gold; Ted Pella).

Ni grids (Formvar/carbon-coated, 200 mesh; Ted Pella) were washed in acetone. Six microliters of Syn5 suspension (2×10^{11} to 3×10^{11} PFU/ml in phage buffer consisting of 50 mM Tris, pH 7.5, 100 mM NaCl, 100 mM $MgCl_2$) was applied per grid and allowed to bind for 10 to 15 min. All subsequent steps were performed with grids floating on the surfaces of convex drops (98 μl) of each successive solution placed in the wells of 96-well plate sealers. The sealers were then enclosed in a plastic box, placed over a sheet of wet blotting paper to minimize evaporation, and gently shaken on a Labnet Model 20 shaker (speed 200). Antibodies were diluted in wash buffer–0.3% cold fish gelatin (Ted Pella) in phage buffer. Blocking was with 3% cold fish gelatin in phage buffer for 30 min at room temperature. The grids were then edge blotted briefly on filter paper and incubated on a drop of wash buffer containing the primary antibody serum. Optimal antibody dilutions (determined empirically) were as follows: anti-gp53, 1:2; anti-gp54, 1:2; anti-gp58, 1:2; and anti-Syn5, 1:100. As a negative control, grids with Syn5 particles were incubated with the preimmunization serum of each antibody at a dilution of 1:2. Incubation with primary antibodies was for 30 min at 37°C. For the wash step, the grids were edge blotted briefly on filter paper and floated three times for 10 min (each) on drops of wash buffer, with no blotting between the wash steps but with blotting before incubation with the secondary antibodies. The secondary antibodies were used at 1:100 dilutions and under the same incubation conditions as used with the primary antibodies. The wash step was repeated in buffer, followed by a final wash step in MilliQ water for 15 min prior to staining with uranyl acetate.

Sucrose gradients of the recombinant proteins gp53 and gp54. The purified recombinant proteins (100 μl of 0.3 to 0.4 mg/ml stocks) were loaded in 5-ml, 5 to 20% continuous sucrose gradients prepared in protein storage buffer (25 mM Tris, pH 7.5, 100 mM NaCl, and 2 mM EDTA) and spun at 218,500 × *g* for 6 h at 4°C in a SW55 Ti Beckman rotor. The gradients were collected as 20 fractions using a gradient fractionator (BioComp Instruments). Aliquots of each fraction were mixed with SDS loading dye, loaded on a 12% SDS-PAGE gel, electrophoresed for 2 h at 13 V/cm, stained with Krypton (Pierce), and scanned on a Typhoon 9400. Gradient fractions of interest were collected and dialyzed to reduce the amount of sucrose. The samples were concentrated in a Vivaspin 10,000-molecular-weight-cutoff (MWCO)filter (Sartorius Stedim) for gp53 and in an Amicon 30,000-MWCO filter (Millipore) for gp54. To determine the S values of gp53 and gp54, catalase, RubisCo (ribulose 1,5-bisphosphate carboxylase/oxygenase), and P22 tail spike were centrifuged in gradients under the same conditions as gp53 and gp54 and used to calibrate sedimentation values. The gp54 peak in the sucrose gradient was within the standards range while the gp53 value was extrapolated from the standard curve.

Syn5 inactivation with anti-Syn5, anti-gp53, and anti-gp54 sera. For this experiment, a fresh stock of Syn5 with the infectivity of 10^{11} PFU/ml was diluted in fresh buffer, titers were determined, and the dilution with a titer of 10^6 PFU/ml was used for the experiment. Based on the experimental procedure, the majority of the particles were infectious.

Growing host cells for plating (3×10^8 to 4×10^8 cells/ml) were diluted 2-fold into fresh artificial seawater (ASW) medium the day before the experiment and incubated overnight (8). Four serum dilutions (1:200, 1:2,000, 1:20,000, and 1:200,000) were prepared for each antibody—anti-Syn5, anti-gp53, and anti-gp54. CsCl-purified Syn5 phage (0.1 ml of 3×10^6 PFU/ml in phage buffer) was added to 0.9 ml of each serum dilution and incubated for 1 h at 37°C in a water bath. To stop each reaction, 0.1 ml of the phage-serum mixture was added to 9.9 ml of room temperature phage buffer. From the diluted mixture, additional serial dilutions were prepared, if needed, for plating. Different volumes of each dilution were mixed with 1 ml of host cells and held for 1 to 2 min to allow phage adsorption to the cells. About 3.5 ml of melted agar at 32°C (1% low-melting-point [LMP] agarose in ASW) was added to each host-phage dilution, and the contents of the entire tube were poured into a petri plate (51 mm). The plates were incubated in a Percival light incubator with continuous irradiation of about 40 μmol of photons per m^{-2} s^{-1} at 28°C, and PFU were counted after incubation overnight.

To test for the efficiency of immunoprecipitation with anti-gp53 and anti-gp54 antibodies, Syn5 particles (50 μl; 10^{11} PFU/ml) were incubated separately with antibodies (2.5 μl of anti-Syn5 and 2.5 μl of a mixture of anti-gp53 and anti-gp54) overnight at 4°C. Samples were centrifuged at 12,000 × *g* for 5 min; the supernatant was separated from the pellet and electrophoresed on an SDS-PAGE gel. The gel was stained with Krypton (Pierce).

Radioactive labeling of phage proteins during Syn5 infection. Growing host cells at 2×10^8 to 5×10^8 cells/ml were diluted about 2-fold into fresh ASW at 24 to 48 h prior to the experiment and incubated overnight.

The culture (1 liter) was infected with Syn5 at a multiplicity of infection (MOI) of 3 to 5. At 25 min after infection, a mixture of 10 μCi/ml [^{35}S]Met-Cys and 100 μCi/ml ^{14}C-labeled amino acids (Perkin-Elmer/NEN) was added. Labeling was allowed to proceed for 10 min, and the culture was chased at 35 min with an amino acid mixture (40 ml per 600-ml culture of (RPMI 1640 Amino Acid mix [Sigma] supplemented with 20 mM L-Met, 20 mM L-Cys, and 47 mM L-Ala). When Casamino Acids were used instead of the amino acid mix, the Syn5 scaffolding protein (gp38) was not detected in either the labeled sample or the unlabeled control. The experiments were conducted at 28°C in a shaking (ca. 200 rpm) water bath under the illumination of a cool-white fluorescent lamp with irradiation of 30 to 40 μmol of photons per m^{-2} s^{-1} at the water surface. Under these conditions the eclipse period was about 55 min, and the latent period was about 85 min. The cells were harvested at 70 min since this time point was determined empirically to give the best procapsid yield. After collection, the cells were held on ice for 10 min, centrifuged at 9,000 × *g* for 10 min at 4°C, resuspended in 100 mM NaCl and 50 mM Tris (pH 7.5) supplemented with Roche protease inhibitor (Mini Tablets, EDTA-free; one tablet per 7 ml of buffer), concentrated 1,000-fold, and stored at −20°C.

The pellets were thawed on ice and then lysed in the presence of 2 mg/ml lysozyme for 30 min at room temperature. DNase I (Worthington) was added at a final concentration of 1 μg/μl, and the samples were mixed for 30 min at room temperature. The supernatants were separated from the debris by spinning at 10,000 × *g* for 10 min at 4°C.

Sucrose gradients (continuous 5 to 20%, with a bottom shelf of 200 μl of 60% sucrose) were prepared, run at 167,300 × *g* (SW55 rotor; Beckman) for 45 min, and collected under the same conditions described above for the sucrose gradients of the recombinant proteins. Aliquots for SDS-PAGE (30 μl) were mixed with 1/2 volume of sample buffer (188 mM Tris [pH 6.8], 2% SDS, 15% β-mercaptoethanol, and bromophenol blue) and heated at 95°C for 5 to 10 min. The discontinuous buffer system of King and Laemmli was used with a Bio-Rad Criterion Gel Cassette system. The gels were electrophoresed for 2 h at about 13 V/cm. Radioactive gels were exposed to a phosphor plate, and a Typhoon 9400 imager was used to scan the plate. Bands were quantified by a GelAnalyzer in conjunction with ImageJ software (13).

To better quantify the proteins in the peaks of the intermediate assembly particles, an additional sucrose gradient was performed using a sample from the same pulse-chase experiment (5 to 45% sucrose; centrifugation at 167,300 × *g* in an SW41 rotor [Beckman] for 45 min). Fractions in the region of interest (fractions 5 to 15) were applied to a 12-well gel so that larger samples (40 μl) could be loaded and analyzed.

Electron microscopy. All grids were stained by flotation on a drop of 1% uranyl acetate for 30 to 60 s, edge blotted with filter paper, and air dried for about 30 min. The grids were observed under a JEOL 1200 transmission electron microscope (TEM) at 60 kV. Images were recorded with an Advanced Microscopy Techniques (AMT) XR41S side-mounted charge-coupled-device (CCD) camera and saved as TIFF files.

RESULTS

Location of the novel proteins in phage particles. To investigate which novel proteins might contribute to specific Syn5 structures, primary antibodies raised against intact infectious particles and against each of the novel proteins—gp53 (~48 kDa), gp54 (~65 kDa), and gp58 (16.6 kDa)—were used in immunogold labeling experiments. Purified virions were incubated with the primary rabbit antibodies and then with goat anti-rabbit secondary antibodies, and the resulting complexes were visualized by negative staining in an electron microscope. To assess the distribution of gold beads associated with the virions, the following criteria were applied. Grid areas with low background labeling were chosen (fewer than five beads on the grid surface in an image at a magnification of ×120,000), and only full phage particles lying entirely within the field of the micrograph were considered. Only gold labels located 20 to 25 nm or less from the phage surface were included as this distance is estimated to be the maximum that a bead would be positioned considering the combined lengths of complexes of primary and secondary antibodies.

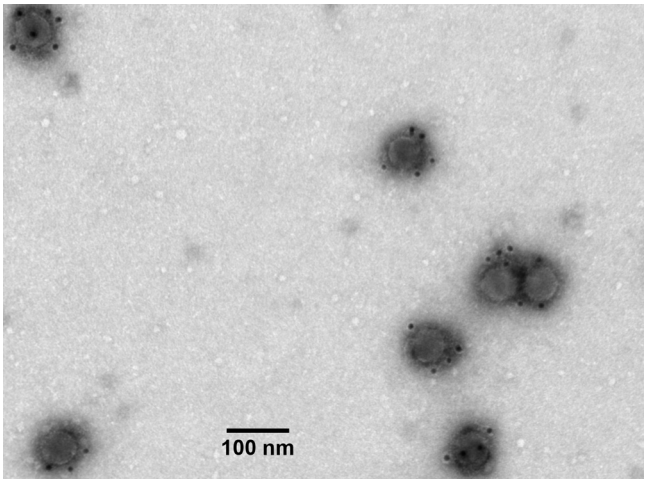

FIG 2 Labeling of Syn5 with anti-Syn5 antibodies. Magnification, ×120,000.

Cryo-electron microscopy (Fig. 1A) has shown that the Syn5 horn is always positioned at the vertex opposite the tail (7). Thus, only particles where the tail vertex could be identified were included in the data collection in order to reduce ambiguity about the positions of the gold beads. In summarizing the data, the phage particle vertices were designated as shown in Fig. 1B, and the beads labeling the particles were assigned positions accordingly.

To assess the percentage of nonspecific labeling, preimmunization rabbit serum for each primary antibody was used as a primary antibody in labeling Syn5 virions (negative control). Nonspecific labeling was estimated to be about 3.5%.

As a positive control, we used anti-Syn5 antibodies raised in rabbits against whole virion particles (Fig. 2). Most of the particles were associated with numerous gold beads distributed randomly over the entire particle surface. Most of them likely represent antibody binding to the coat, the major structural protein of the virions.

The first possible horn protein to be examined was gp53 (48 kDa). Labeled particles are shown in Fig. 3, and the collected data are summarized in Table 1. By cryo-EM (Fig. 1A) the Syn5 horn (about 30 to 35 nm long) points perpendicularly away from the phage or, more often, is tilted at the base and points toward the sides of the phage particle (Fig. 1B, vertices 3). In addition to the horn flexibility, the primary and secondary antibody complexes can have lengths of 20 to 25 nm, so the gold bead can be positioned up to 25 nm away from the target. Thus, if gp53 is a horn protein, the gold labels should be located at and around vertices 2 and 3. As seen in Table 1, about 90% of the labels are at vertices 2 and 3 (~12% and 38%) and between the two (~38%). About 7% of the labels are between vertices 3 and 4. About 4% are at other positions, in close agreement with the 3.5% estimate for nonspecific labeling. In numerous particles, clusters of gold beads were observed between vertices 2 and 3 (Fig. 3), where the horn is apparently attached. Taken together, the data suggest that gp53 forms

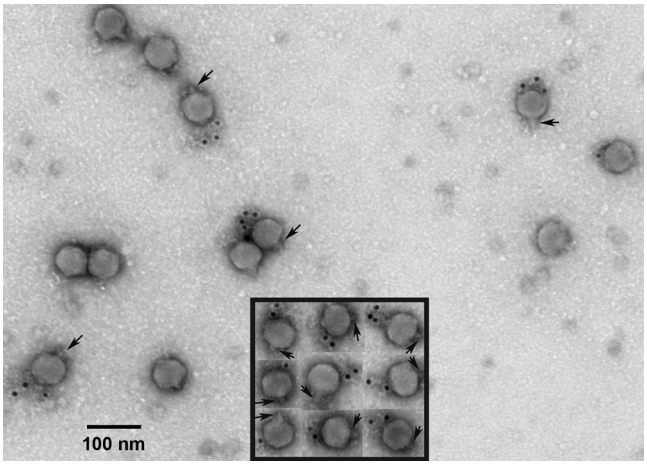

FIG 3 Labeling of Syn5 with anti-gp53 antibodies. The image shows a characteristic labeling pattern with anti-gp53 antibodies (magnification, ×120,000). The inset contains selected labeled single particles from other images. Black arrows indicate the tails.

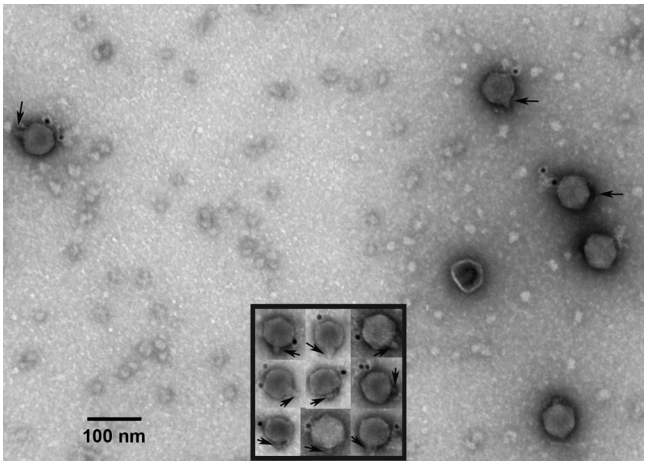

FIG 4 Labeling of Syn5 with anti-gp54 antibodies. The image shows a characteristic labeling pattern with anti-gp54 antibodies (magnification, ×120,000). The inset contains selected labeled single particles from other images. Black arrows indicate the tails.

the shaft of the horn or at least is present along the length of the horn.

The second possible horn protein, gp54 (65 kDa), was investigated by labeling phage particles with anti-gp54 primary antibodies. The labeling pattern was different from that of gp53. The gold beads were most often (84%) observed at and around vertex 3 (Fig. 4 and Table 1), with ~44% at vertex 3, ~33% between vertices 3 and 4, and 7% between vertices 2 and 3. About 11% of gold beads were at vertex 2. The labeling at other positions was approximately 5%, similar to the results for false-positive labels. Clusters of gold beads in the area of the presumed horn position were rarely observed, and even in those cases there were usually no more than two beads present.

The labeling distribution for gp54 suggests that this is also a horn protein, but it builds a different component of the horn than gp53. While gp53 labels are at and around vertices 2 and 3, the labels of gp54 are at and around vertex 3, more distant from the horn base at vertex 2. The high proportion of labels at and around vertex 3 suggests that gp54 may be a structural component of the tip of the horn. There are estimated to be only six copies of gp54 per virion, which may explain the lack of large bead clusters with anti-gp54 antibodies. Another reason might be that gp54 builds a smaller part of the horn.

The data for the third Syn5 novel protein, gp58 (16 kDa) (Fig. 5) (153 beads associated with 104 virions) produced a very different pattern from the patterns for gp53 and gp54. About half of the beads (~50%) were distributed between pentamer vertices (consistent with the positions of the hexamers). The majority of the other 50% were at vertices 3 (~15%) and 4 (~27%), with very few labels on vertices 1 (the tail vertex, ~3%) and 2 (the horn vertex, ~5%). If gp58 is a hexamer knob protein, then the labels should be found between pentamer vertices (1 and 4, 3 and 4, and 2 and 3), which is consistent with the data. Labels at vertices 3 and 4 are probably due to the extended length of the primary and secondary antibody complexes. Few labels are observed at the portal and horn vertices, probably due to spatial interference of the horn and the tail. Since anti-gp58 antibodies do not recognize the coat protein (12), it is reasonable to conclude that the virion components labeled by the anti-gp58 antibodies are the hexamer knobs and that gp58 is an outer capsid protein.

The recombinant horn proteins exhibit complex polymerized structures. Once gp53 and gp54 were designated putative horn proteins, the question of how they contribute to the assembly of the horn appendage could be addressed. Estimates of the abundance of the two proteins upon SDS-PAGE fractionation of Syn5 particles indicated that there are about 12 copies of gp53 and 6 copies of gp54 per virion. In sucrose gradients, the sedimentation coefficients of the recombinant proteins were estimated to be 43S for gp53 and 6S for gp54. Gradient fractions of the peaks for each protein were assessed by electron microscopy (Fig. 6). The images revealed very long, fibrous structures in the gp53 samples. In the case of gp54, numerous short rod-shaped structures were observed. Both protein samples were filtered prior to sedimentation, but there is a possibility that the complex formations observed are the result of aggregates.

Will Syn5 virions infect the host after treatment with anti-horn antibodies? It is well known that serum raised against intact virions can block phage infectivity (14, 15). A plausible hypothesis

TABLE 1 Summary data with the positions of anti-gp53 and anti-gp54 gold labels on the Syn5 surface

Antibody	No. of counted particles	Total no. of total gold labels	Label frequency (% [no. of labels])[a]				
			On vertex 2	On vertex 3	Between vertices 2 and 3	Between vertices 3 and 4	Other
Anti-gp53	126	146	~12 (18)	~38 (56)	~38 (56)	~7 (10)	~4 (6)
Anti-gp54	126	152	~11 (16)	~44 (67)	~7 (11)	~33 (50)	~5 (8)

[a] Percentages are determined relative to the total number of gold labels for the respective antibody.

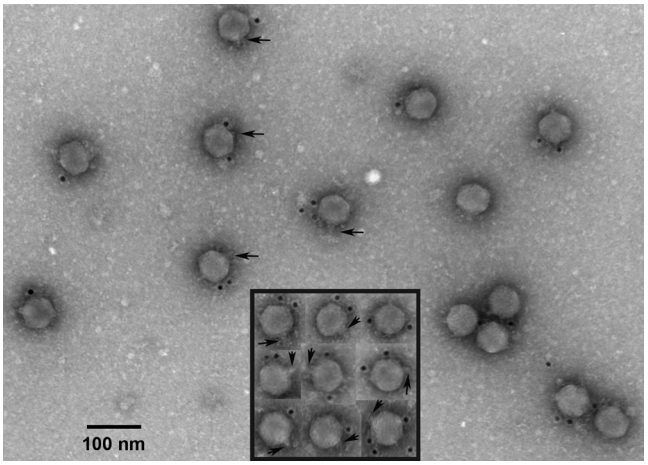

FIG 5 Labeling of Syn5 with anti-gp58 antibodies. The image shows a typical labeling pattern with anti-gp58 antibodies (magnification, ×120,000). The inset contains selected labeled single particles from other images. Black arrows indicate the tails.

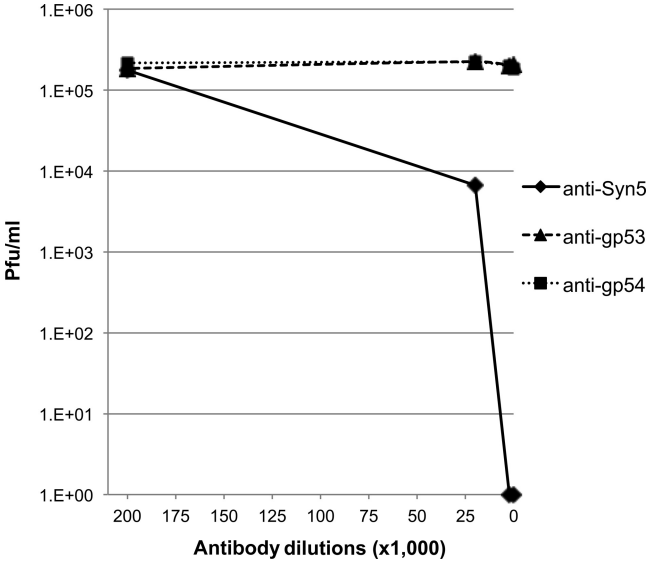

FIG 7 Effect of anti-Syn5, anti-gp53, and anti-gp54 antibodies on Syn5 infectivity.

for the function of the Syn5 horn is that it is used by the phage to infect the host. This is the case for the head appendages of the *Caulobacter* phages Cb13 and CbK (16).

Since our data suggest that gp53 (48 kDa) and gp54 (65 kDa) are horn proteins, we tested whether the antibodies used for their identification could reduce or block the infectivity of Syn5. Syn5 infectious particles were mixed with either anti-gp53 or anti-gp54 antibodies at a range of dilutions and incubated for 1 h at 37°C, and plaque assays were performed. As a positive control, anti-Syn5 serum raised against whole viral particles was also tested. The anti-Syn5 serum contains antibodies against all of the external proteins of Syn5, and some bind strongly to the putative tail fiber protein of Syn5 (gp46) (8).

As seen in Fig. 7, the anti-Syn5 antibodies inactivated the Syn5 infectious particles completely at serum dilutions of 1:2,000 and 1:200, partially at a dilution of 1:20,000, but not at 1:200,000. On the other hand, when infectious virions were treated with anti-gp53 or anti-gp54 antibodies, the phage titers remained unchanged at all dilutions tested. This lack of effect on Syn5 infectivity suggests that the horn structure of Syn5 may not be needed for infection of the laboratory host *Synechococcus* sp. WH8109.

The anti-gp53 and anti-gp54 antibodies were raised against the recombinant proteins while the anti-Syn5 antibodies were raised against the whole virion. Immunoprecipitation of infectious particles was performed with anti-Syn5 antibodies and a mixture of anti-gp53 and anti-gp54 (dilution factors were the same for anti-Syn5 and the mix) (data not shown). The precipitated particles were separated from the unprecipitated ones by centrifugation. The results indicate that the mixture of antibodies raised against the recombinant proteins and the anti-Syn5 antibodies precipitated Syn5 particles with almost equal efficiency.

Protein composition of precursor particles during virion assembly. As reported earlier, Syn5 assembles through a procapsid intermediate, and two classes of procapsids, 240S and 340S, were

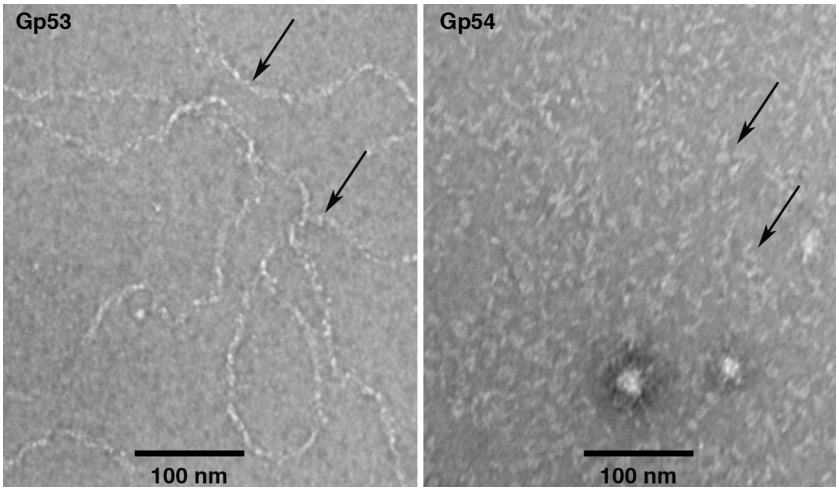

FIG 6 Electron micrographs of recombinant gp53 and gp54. The images show sucrose gradient fractions of gp53 and gp54. Samples were negatively stained with 1% uranyl acetate and observed at a magnification of ×150,000. Black arrows indicate the protein structures.

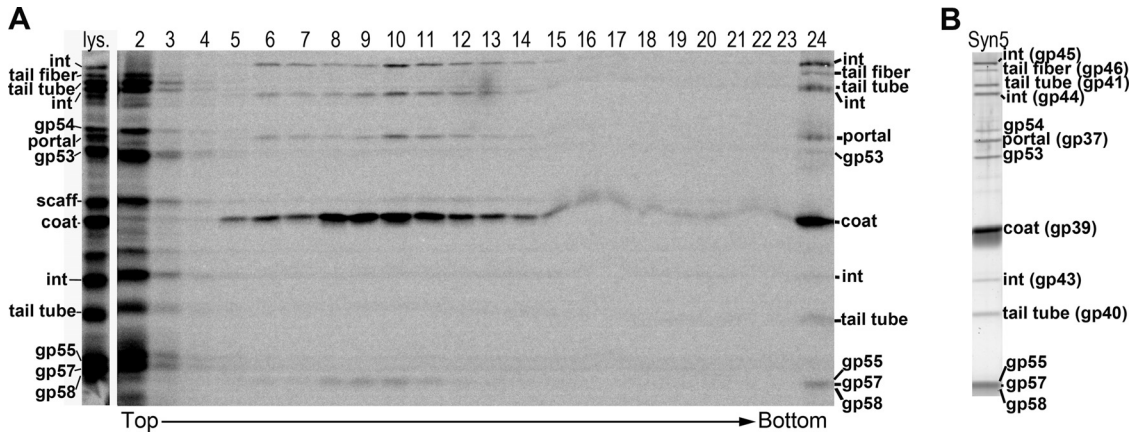

FIG 8 Radiolabeling of Syn5 proteins during infection. (A) SDS-PAGE gel of fractionated sucrose gradients of supernatants of lysed cells labeled with a mixture of ^{14}C-labeled amino acids during Syn5 infection (25 to 35 min postinfection). The cells were concentrated 1,000-fold before lysis. The gel was exposed for imaging for 22 days. Lys, whole-cell lysate; int, internal protein; scaff, scaffolding protein. (B) SDS-PAGE of purified infectious Syn5 virions (Krypton stained) included here for comparison of the protein profile to the radiolabeled proteins.

identified by their sedimentation coefficients and the presence of coat and scaffolding proteins (8). Recently, using high-resolution cryo-electron tomography (9), we were able to directly image two distinct classes of shells lacking DNA within the infected *Synechococcus* cytoplasm: procapsids and expanded capsids lacking scaffolding.

To identify minor structural proteins, including the novel proteins, present in Syn5 procapsids, a pulse-chase experiment was performed using radiolabeled amino acids. Proteins newly synthesized during Syn5 infection of the WH8109 host were prepared from cells labeled for 10 min with a mixture of [^{35}S]Met-Cys and ^{14}C-labeled amino acids and fractionated by sucrose gradient, followed by SDS-PAGE. In Fig. 8A, the first lane, representing the total lysate, shows a protein pattern which is a good match to the structural protein profile of infectious Syn5 particles (Fig. 8B).

There was no evidence of protein bands present in the stained gels that were absent from the radiolabeled samples. This argues against the incorporation of preformed host proteins into phage particles. From serial dilutions of gel samples, we estimate that we could have identified a host protein band representing 1 to 2 molecules of a protein of 40,000 Da.

The Syn5 coat is clearly visible throughout the gradient shown in Fig. 8 as the major structural protein, with ~400 copies per particle. As expected, the scaffolding is also present in the labeled lysate but not in the mature virions at the bottom (fraction 24). The top of the gradient (fraction 2) contains all of the free proteins, the middle (fractions 8 to 13) contains procapsids, and the bottom (fraction 24) contains phage particles that have packaged the DNA. The particles that sediment in fractions 10 to 13 contain scaffolding protein—the faint band just above the coat protein—as well as the two major internal proteins, the portal protein, and possibly a small internal protein (gp44). This supports the identification of the particles in fractions 10 to 13 as procapsids (8). Note that the portal protein, which was not confirmed in the study of Raytcheva et al. (8) is clearly present in the radiolabeled procapsids (Fig. 8 and 9).

The particles in fractions 6 to 9 contain the two major internal proteins, gp45 (152 kDa) and gp44 (90 kDa), the portal gp37 protein (60 kDa), one or more of the three small proteins gp55, gp57, and gp58 (~16 kDa), and possibly the small internal protein gp43 (23 kDa). These particles are presumably the expanded procapsids which have lost their scaffolding. There is a faint band of scaffolding protein, but it is not present as a well-defined peak. Its presence seems to be more the result of insufficient resolution of the expanded capsid peaks from the soluble scaffolding protein in the top fractions.

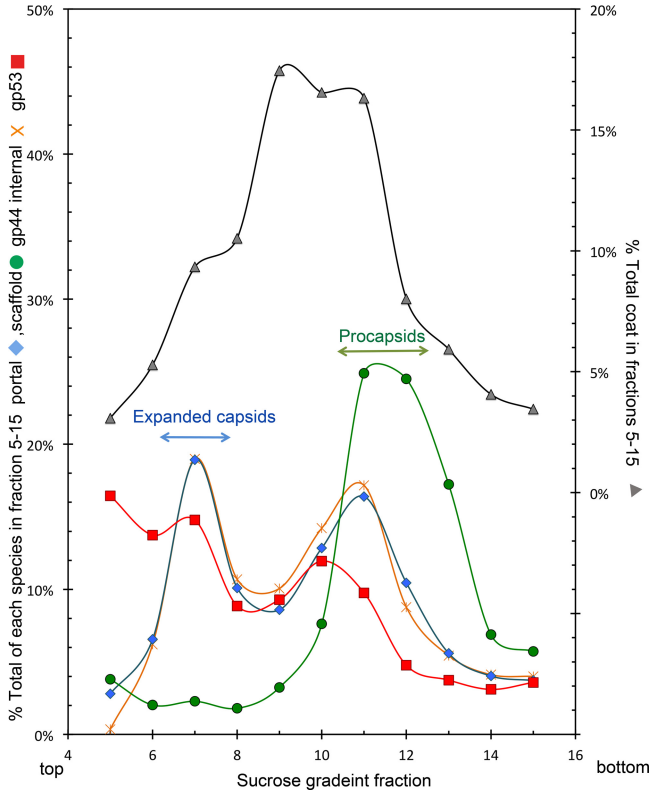

FIG 9 Quantification of a sucrose gradient showing the distribution of Syn5 precursor species. The percent totals of the individual species in fractions 5 to 15 were calculated and plotted against the fractions. Proteins are identified as indicated on their respective axes.

To further resolve and quantify the species of interest, a pulse-chase experiment was performed as described above, and the samples were loaded on a 5 to 45% sucrose gradient in a longer tube. Fractions 5 to 15 were applied to a 12-well SDS-PAGE gel, and the resulting gel was exposed for 12 days. The bands were quantified, and the percent totals of coat, portal, and scaffolding proteins and internal protein gp44 (90 kDa) and putative horn gp53 (48 kDa) in all fractions were plotted against the fraction number (Fig. 9).

The distributions of the scaffolding and portal proteins indicate that the faster-sedimenting (fractions 10 to 13) particles are the procapsids. The trailing (fractions 6 to 8) particles contain the portal but lack the scaffolding protein. The gp44 internal protein, essential for any productive precursors, is present in two major peaks (fractions 6 to 8 and 10 to 13). The increased mass and decreased diameter of procapsids account for their higher sedimentation than expanded procapsids.

The distribution of labeled proteins shown in Fig. 8 and 9 is consistent with the presence of a third class of precursor particles lacking condensed DNA: procapsids in fractions 10 to 13, expanded procapsids in fractions 6 to 8, and a class sedimenting between the two.

A protein band corresponding to the mass of the gp53 horn protein is present in the middle of the gradient, and its distribution shows two peaks; the slower peak (fractions 6 to 8) coincides with the expanded capsids and may represent gp53 assembled onto them. However, since purified gp53 shows a broad sedimentation profile, its association with the expanded capsids remains to be confirmed. The leading edge (fractions 9 to 11) of the gp53 species does not overlap the peak of the scaffolding distribution (fractions 10 to 13). This suggests that gp53 is not present on the procapsids, supporting the same conclusion reached from cryo-ET experiments (9).

The procapsid region of the gradient lacked defined peaks of the horn protein gp53 (48 kDa) or gp54 (65 kDa) although a faint band corresponding to the mass of gp53 is detectable in these fractions. It should be noted that, when centrifuged through a sucrose gradient (under similar conditions as the lysates), recombinant gp53 sedimented throughout the gradient, presumably due to its fiber-like nature. It is possible that the same is true for native gp53. The protein band (~16 kDa) containing one or more of the three Syn5 outer capsid proteins, gp55, gp57, and gp58, cosediments with the coat protein in fractions 8 to 10 (Fig. 8). This suggests that the intermediate particles are closer to mature virions than to procapsids.

DISCUSSION

Composition of the horn and knob-like capsid protrusions. The horn of Syn5 is a distinct morphological feature of this cyanophage. The results from immunogold labeling strongly suggest that gp53 (48 kDa) and gp54 (65 kDa) are components of the horn structure and that they have distinct distributions. Anti-gp53 antibody labeling resulted in gold beads clustered primarily at or near the apparent attachment site of the horn, as seen in cryo-EM images (around the horn vertex 2 and the neighboring vertex 3). For gp54, the labels were more distant from the horn base (vertex 2) and were most pronounced around the neighboring vertex 3. This is consistent with the location of the tip of the horn if the horn were bent at its base and leaning to the side vertices, an arrangement which is often observed. Since cryo-EM images of Syn5 have not revealed any additional structures around vertex 4 and since there are very few gp54 labels at other vertices, the most likely explanation is that gp54 is a component of the horn tip. However, since the frequencies of gold label at the horn base are approximately equal for the two proteins, gp54 may contribute to other parts of the horn besides the tip, or the labels at the base may represent distant labels due to the extended length of the antibodies. There is also a possibility that the horn may be a double-layered structure with gp53 on the outside and gp54 on the inside and extending through the tip.

The analyses of gp53 and gp54 in sucrose gradients and by electron microscopy indicate that the proteins expressed from cloned genes are not in monomeric form. The molecular mass of recombinant gp53 is ~50 kDa, and that of recombinant gp54 is ~67 kDa, indicating that both are too small to be visualized by EM unless the monomers build more complex structures. Their sedimentation coefficients and the presence of visible structures under EM suggest that gp53 and gp54 may form multimers or complexes *in vivo* needed to build and shape the long horn appendage of Syn5. However, we do not know if the conformation of gp53 and gp54 within the horn structure is extended, as in coiled coils, or globular. The Pap pilus of *Escherichia coli* is an elongated organelle of known structure and, therefore, protein density (17). Using that structure as a model and assuming 6-fold rotational symmetry for the horn (Preeti Gipson and Wah Chiu, personal communication), we estimate that the Syn5 horn could be assembled from 12 to 18 copies of gp53 and 6 copies of gp54, consistent with the stoichiometry determined from SDS gel electrophoresis.

One hypothesis for the function of the Syn5 horn is that it is involved in host recognition. This is the case for the *Caulobacter* phages Cb13 and CbK, which have a long head appendage on the vertex opposite the tail and which wrap it tightly around the host flagellum (16). Other phages that use their tails to bind to the host flagella or pili have also been described (18–21). However, attempts to lower or block phage infectivity using antibodies against the horn proteins (anti-gp53 and anti-gp54) were unsuccessful (Fig. 7). One possible explanation is that the horn is not involved in host recognition or attachment in the infection process but, instead, has a different function. Alternatively, it may be involved in host attachment but to a host other than *Synechococcus* sp. WH8109. This cyanobacterial species is the only known lytic host identified to date for Syn5; at least 19 other cyanobacterial species have failed to exhibit lysis triggered by Syn5 (5, 6). *Synechococcus* sp. WH8109 is nonmotile, and, in general, motile *Synechococcus* cyanobacteria do not possess flagella or pili (22). Novel putative swimming structures for *Synechococcus* have been described in strain WH8113 (23).

It is also possible that the horn is used for attachment, not to the bacterial host but to other particulates in the water, which might keep the phage in nutrient-rich waters and hence closer to its host(s). Finally, it remains possible that the horn does assist Syn5 in the attachment steps, but since the antibodies utilized in the phage-inactivating experiment were raised against recombinant proteins and not against the horn appendages in their native forms, they may not be efficient in binding to the horn epitopes of the mature phage responsible for attaching to the bacterial host even though they were successfully used for labeling the horn. However, a mixture of the anti-gp53 and anti-gp54 antibodies was

almost as efficient as anti-Syn5 antibodies in precipitating infectious Syn5 particles (data not shown).

Each Syn5 capsid hexamer carries three knob-like protrusions, presumably outer capsid proteins. In the 18-Å resolution structure in Pope et al. (7), there was no indication of distinct decoration proteins. From structures resolved to 5 Å, the protrusions turned out to be separate molecules from the major capsid subunit (Gipson and Chiu, personal communication). The pattern of the gold labeling with anti-gp58 antibodies indicates that gp58 is an outer capsid protein. There are three knobs per hexamer, but the resolution of the data does not clarify whether all three knobs are made of gp58. Since Syn5 has two additional structural proteins (gp55 and gp57) of unknown function and about the same mass as gp58, they, too, may contribute to building the outer capsid proteins. The number of molecules of the three combined proteins estimated to be present per virion (from SDS-PAGE) is consistent with the number of hexamer molecules present per virion.

Protein composition of procapsids and capsids. The more slowly sedimenting class of particles resolved in the sucrose gradients are presumably expanded capsids, containing coat and portal proteins, two major internal proteins, and possibly the small internal protein, as well as the three small putative outer capsid proteins. They presumably represent the expanded capsids described by Dai et al. (9). Particles lacking DNA and scaffolding could be kinetic intermediates in DNA packaging and capsid maturation, or they could be particles that initiated DNA packaging inside the cells but lost the DNA after host lysis (24). Such structures have been described in phage P22 (24–26) as well as other phages (27–30). The second class, procapsid particles, contains all the proteins of the expanded capsids with the addition of the scaffolding protein. The putative additional class lacks scaffolding and may represent an intermediate stage in capsid expansion.

The intensity of the scaffolding protein in radiolabeled samples was lower than would be expected for a protein expected to be present at more than 100 molecules/per capsid. In the original report of scaffolding proteins in P22 morphogenesis, the intensity of scaffolding bands was anomalously low (31). This was shown to be due to the recycling of the scaffolding during P22 procapsid assembly. The Syn5 results could be either recycling or degradation. Degradation of the scaffolding in Syn5 has been observed and described in Raytcheva et al. (8).

The ~16-kDa protein gel band cosediments with the expanded capsids but not with the procapsids. One of the proteins present in Syn5 mature virions in this band (gp58) was identified as an outer capsid protein. If gp58 is indeed present on the expanded capsids, then its role may be to stabilize the capsid shell once the scaffolding leaves. The decoration proteins of phage lambda have such a function (32).

The gold-labeling experiments localized gp53 (48 kDa) to the horn shaft. While gp53 is in low abundance in the radiolabeled particles, it appears to be associated with both the trailing edge of the procapsids and with the expanded capsids. Since gp53 forms a portion of the horn shaft but does not track with the scaffolding, it is most likely not present on procapsids. The assembly of the horn may begin after scaffolding release. It should be noted that recombinant gp53 sediments throughout the sucrose gradient when it is run under similar conditions. It is possible that the gp53 proteins associated with the peaks of the precursor particles are an artifact of the free gp53 protein polymers. The cryo-ET of Dai et al. (9) did not reveal a complete horn structure on the procapsid or the expanded capsid.

The second horn protein gp54 (65 kDa) did not appear to be associated with the precursor particles. The assembly of the Syn5 horn proteins on a single vertex of the mature virion opposite the tail requires the selection of only one of the sets of 11 quasi-equivalent 5-fold vertices. Phage tail structures attach to proteins interacting with the unique portal vertex. It will be important to determine what distinguishes the vertex opposite the portal vertex in Syn5 for horn assembly.

To date, all phages described which carry structures located on the vertex opposite the tail infect aquatic prokaryotes. This raises the possibility that such structures may not be an exception in hosts inhabiting the dilute water environments. Encounters between phages and their hosts probably happen relatively rarely in these ecosystems, and the phages may have evolved structures to facilitate the process. It is also plausible that the phages use these structures to attach to other organisms or to debris to reside closer to nutrient- and host-rich areas.

ACKNOWLEDGMENTS

We thank Preeti Gipson (Baylor College of Medicine) for kindly providing the cryo-EM image of Syn5. We thank Bill Fowle (Northeastern University) and Wei Dai (Baylor College of Medicine) for ideas and suggestions about the immunogold labeling experiments.

This work was partially supported by NIH grants GM17980 and AI075208 awarded to J.A.K. and by the Department of Biology, Northeastern University.

REFERENCES

1. **Shan J, Jia Y, Clokie MR, Mann NH.** 2008. Infection by the "photosynthetic" phage S-PM2 induces increased synthesis of phycoerythrin in *Synechococcus* sp. WH7803. FEMS Microbiol. Lett. **283:**154–161. http://dx.doi.org/10.1111/j.1574-6968.2008.01148.x.
2. **Lindell D, Jaffe JD, Johnson ZI, Church GM, Chisholm SW.** 2005. Photosynthesis genes in marine viruses yield proteins during host infection. Nature **438:**86–89. http://dx.doi.org/10.1038/nature04111.
3. **Huiskonen JT, Kivela HM, Bamford DH, Butcher SJ.** 2004. The PM2 virion has a novel organization with an internal membrane and pentameric receptor binding spikes. Nat. Struct. Mol. Biol. **11:**850–856. http://dx.doi.org/10.1038/nsmb807.
4. **Huiskonen JT, Manole V, Butcher SJ.** 2007. Tale of two spikes in bacteriophage PRD1. Proc. Natl. Acad. Sci. U. S. A. **104:**6666–6671. http://dx.doi.org/10.1073/pnas.0608625104.
5. **Waterbury JB, Valois FW.** 1993. Resistance to co-occurring phages enables marine *Synechococcus* communities to coexist with cyanophages abundant in seawater. Appl. Environ. Microbiol. **59:**3393–3399.
6. **Sullivan MB, Waterbury JB, Chisholm SW.** 2003. Cyanophages infecting the oceanic cyanobacterium *Prochlorococcus*. Nature **424:**1047–1051. http://dx.doi.org/10.1038/nature01929.
7. **Pope WH, Weigele PR, Chang J, Pedulla ML, Ford ME, Houtz JM, Jiang W, Chiu W, Hatfull GF, Hendrix RW, King J.** 2007. Genome sequence, structural proteins, and capsid organization of the cyanophage Syn5: a "horned" bacteriophage of marine *Synechococcus*. J. Mol. Biol. **368:**966–981. http://dx.doi.org/10.1016/j.jmb.2007.02.046.
8. **Raytcheva DA, Haase-Pettingell C, Piret JM, King JA.** 2011. Intracellular assembly of cyanophage Syn5 proceeds through a scaffold-containing procapsid. J. Virol. **85:**2406–2415. http://dx.doi.org/10.1128/JVI.01601-10.
9. **Dai W, Fu C, Raytcheva D, Flanagan J, Khant HA, Liu X, Rochat RH, Haase-Pettingell C, Piret J, Ludtke SJ, Nagayama K, Schmid MF, King JA, Chiu W.** 2013. Visualizing virus assembly intermediates inside marine cyanobacteria. Nature **502:**707–710. http://dx.doi.org/10.1038/nature12604.
10. **Summons RE, Jahnke LL, Hope JM, Logan GA.** 1999. 2-Methylhopanoids as biomarkers for cyanobacterial oxygenic photosynthesis. Nature **400:**554–557. http://dx.doi.org/10.1038/23005.
11. **Lake JA, Leonard KR.** 1974. Bacteriophage structure: determination of head-tail symmetry mismatch for *Caulobacter crescentus* phage phiCbK. Science **183:**744–747. http://dx.doi.org/10.1126/science.183.4126.744.

12. **Raytcheva DA.** 2012. Ph.D. thesis. Northeastern University, Boston, MA.
13. **Simkovsky R, King J.** 2006. An elongated spine of buried core residues necessary for in vivo folding of the parallel beta-helix of P22 tailspike adhesin. Proc. Natl. Acad. Sci. U. S. A. **103:**3575–3580. http://dx.doi.org/10.1073/pnas.0509087103.
14. **Edgar RS, Lielausis I.** 1964. Temperature-sensitive mutants of bacteriophage T4D: their isolation and genetic characterization. Genetics **49:**649–662.
15. **King J, Wood WB.** 1969. Assembly of bacteriophage T4 tail fibers the sequence of product interactions. J. Mol. Biol. **39:**583–601. http://dx.doi.org/10.1016/0022-2836(69)90147-8.
16. **Guerrero-Ferreira RC, Viollier PH, Ely B, Poindexter JS, Georgieva M, Jensen GJ, Wright ER.** 2011. Alternative mechanism for bacteriophage adsorption to the motile bacterium *Caulobacter crescentus*. Proc. Natl. Acad. Sci. U. S. A. **108:**9963–9968. http://dx.doi.org/10.1073/pnas.1012388108.
17. **Bullitt E, Makowski L.** 1995. Structural polymorphism of bacterial adhesion pili. Nature **373:**164–167. http://dx.doi.org/10.1038/373164a0.
18. **Lotz W, Acker G, Schmitt R.** 1977. Bacteriophage 7-7-1 adsorbs to the complex flagella of *Rhizobium lupini* H13-3. J. Gen. Virol. **34:**9–17. http://dx.doi.org/10.1099/0022-1317-34-1-9.
19. **Schade SZ, Adler J, Ris H.** 1967. How bacteriophage chi attacks motile bacteria. J. Virol. **1:**599–609.
20. **Scholl DR, Jollick JD.** 1980. Pilus-dependent, double-stranded DNA bacteriophage for *Caulobacter*. J. Virol. **35:**949–954.
21. **Wilson JJ, Takahashi I.** 1978. Adsorption of *Bacillus subtilis* bacteriophage PBS 1. Can. J. Microbiol. **24:**1–8. http://dx.doi.org/10.1139/m78-001.
22. **Brahamsha B.** 1999. Non-flagellar swimming in marine *Synechococcus*. J. Mol. Microbiol. Biotechnol. **1:**59–62.
23. **Samuel AD, Petersen JD, Reese TS.** 2001. Envelope structure of *Synechococcus* sp. WH8113, a nonflagellated swimming cyanobacterium. BMC Microbiol. **1:**4. http://dx.doi.org/10.1186/1471-2180-1-4.
24. **Strauss H, King J.** 1984. Steps in the stabilization of newly packaged DNA during phage P22 morphogenesis. J. Mol. Biol. **172:**523–543. http://dx.doi.org/10.1016/S0022-2836(84)80021-2.
25. **King J, Lenk EV, Botstein D.** 1973. Mechanism of head assembly and DNA encapsulation in *Salmonella* phage P22. II. Morphogenetic pathway. J. Mol. Biol. **80:**697–731.
26. **Poteete AR, King J.** 1977. Functions of two new genes in *Salmonella* phage P22 assembly. Virology **76:**725–739. http://dx.doi.org/10.1016/0042-6822(77)90254-9.
27. **Aksyuk AA, Rossmann MG.** 2011. Bacteriophage assembly. Viruses **3:**172–203. http://dx.doi.org/10.3390/v3030172.
28. **Studier FW.** 1972. Bacteriophage T7. Science **176:**367–376. http://dx.doi.org/10.1126/science.176.4033.367.
29. **Studier FW, Maizel JV, Jr.** 1969. T7-directed protein synthesis. Virology **39:**575–586. http://dx.doi.org/10.1016/0042-6822(69)90105-6.
30. **Preux O, Durand D, Huet A, Conway JF, Bertin A, Boulogne C, Drouin-Wahbi J, Trevarin D, Perez J, Vachette P, Boulanger P.** 2013. A two-state cooperative expansion converts the procapsid shell of bacteriophage T5 into a highly stable capsid isomorphous to the final virion head. J. Mol. Biol. **425:**1999–2014. http://dx.doi.org/10.1016/j.jmb.2013.03.002.
31. **King J, Casjens S.** 1974. Catalytic head assembling protein In virus morphogenesis. Nature **251:**112–118. http://dx.doi.org/10.1038/251112a0.
32. **Yang Q, Maluf NK, Catalano CE.** 2008. Packaging of a unit-length viral genome: the role of nucleotides and the gpD decoration protein in stable nucleocapsid assembly in bacteriophage lambda. J. Mol. Biol. **383:**1037–1048. http://dx.doi.org/10.1016/j.jmb.2008.08.063.